AGU ADVANCING EARTH AND SPACE SCIENCE

Geophysical Research Letters

RESEARCH LETTER
10.1029/2020GL090682

On the Estimation of In-Cloud Vertical Air Motion Using Radar Doppler Spectra

Zeen Zhu[1], Pavlos Kollias[1,2], Fan Yang[2], and Edward Luke[2]

[1]School of Marine and Atmospheric Sciences, Stony Brook University, Stony Brook, NY, USA, [2]Environmental and Climate Sciences Department, Brookhaven National Laboratory Upton, NY, USA

Key Points:

- A new, unbiased retrieval technique for the estimation of the vertical air motion in clouds based on radar Doppler spectra is presented
- Comparison with independent measurements and simulations indicates that the retrieval technique is unbiased
- The air motion retrieval can be used to characterize the updraft and downdraft motions in clouds as a function of environmental parameters

Supporting Information:

- Supporting Information S1

Correspondence to:
Z. Zhu,
zeen.zhu@stonybrook.edu

Citation:
Zhu, Z., Kollias, P., Yang, F., & Luke, E. (2021). On the estimation of in-cloud vertical air motion using radar Doppler spectra. *Geophysical Research Letters*, *48*, e2020GL090682. https://doi.org/10.1029/2020GL090682

Received 5 SEP 2020
Accepted 19 NOV 2020

Abstract Measurements of in-cloud vertical air motion are key to quantitatively describe cloud dynamics and their role in cloud microphysics. Here, a retrieval technique for estimating the in-cloud vertical air motion using the upward edge of the radar Doppler spectrum is presented. An additional broadening correction factor that depends on the signal-to-noise ratio (SNR) is introduced. A variety of independent measurements are used to assess the performance of the new technique. The vertical air motion is unbiased with an uncertainty of 0.2 m s^{-1} for SNR <30. The properties of in-cloud vertical air motion are investigated from 1 year of ground-based observations of warm marine boundary layer clouds. Clouds with higher LWP are characterized by stronger vertical air motions compared to those having lower LWP values.

Plain Language Summary Knowledge of the strength of updrafts and downdrafts in clouds is important for understanding the role of cloud dynamics on cloud lifetime. Short-wavelength radars are capable of detecting and penetrating clouds; however, the use of the Doppler velocity to estimate the vertical air motion is not straightforward, due to the contribution of the particle sedimentation velocity. Here, a previously proposed technique is revisited, and a crucial correction is introduced. The improved retrieval technique provides unbiased vertical air motion estimates with an uncertainty of 0.2 m s^{-1}. The technique is applicable to both stratiform and cumulus clouds with and without precipitation.

1. Introduction

In-cloud vertical air motion (V_{air}) is a key parameter for determining the strength of convection, the vertical transport of heat and moisture, and entrainment rate (Donner et al., 2016). These processes affect cloud fraction and lifetime (Park et al., 2016). Measurements of V_{air} are necessary for characterizing the dynamical structure of clouds (Blyth et al., 2005; Kollias et al., 2001) and its impact on cloud microphysics (Kollias et al., 2003; Korolev & Isaac, 2003; Takahashi et al., 2017). The vertical air motion statistics are also important in model parameterization schemes as it relates to the cloud base buoyancy and entrainment rate (Bretherton et al., 2004; de Roode et al., 2012).

Despite their importance, in-cloud V_{air} measurements are sparse, especially in shallow convection. Aircraft-based in situ V_{air} measurements are of high quality but limited to the flight level during field campaigns (Telford & Warner, 1962; Wang et al., 2012). Surface-based Doppler lidars have proven to be very useful in providing V_{air} measurements in the subcloud layer (Ansmann et al., 2010; Lamer & Kollias, 2015; Lareau et al., 2018). Profiling Doppler radars, especially mm-wavelength radars have the ability to both detect and penetrate clouds and thus, provide detailed information on cloud dynamics (Kollias et al., 2007a). When pointing vertically, the observed radar Doppler velocity V_d is the sum of the V_{air} and the reflectivity-weighted particle size distribution (PSD) sedimentation velocity V_{sed}. To separate these two velocity contributions, assumptions are needed. One widely used decomposition technique is to assume that over a long temporal averaging period (20–60 min) the mean V_{air} is zero. Using this assumption, empirical relationships between the radar reflectivity factor (Z) and V_{sed} can be constructed and the residual vertical air motion can be retrieved as $V_{air} = V_d - V_{sed}(Z)$ (Delanoe et al., 2007; Kalesse & Kollias, 2013; Protat & Williams, 2011). However, this approach is only valid in nonconvective regimes (e.g., cirrus clouds and large-scale stratiform precipitation). Another approach is to assume that $V_{air} = V_d$ (Gossard, 1994; Kollias et al., 2001). This assumption is valid in nonprecipitating clouds $V_{sed} \approx 0$.

If the entire radar Doppler spectrum is available, several additional techniques have been proposed. In particular, Wakasugi et al. (1986) and Williams (2012) utilized radar Doppler spectra from radar wind profilers (RWPs) to estimate V_{air}, and more recently, Radenz et al. (2018) combined spectra from an RWP and a cloud radar to estimate in-cloud vertical motion. In particular, RWPs operating in the VHF (50 and 400 MHz) bands can directly provide vertical air motion estimates using Bragg scattering from clear-air refractive index irregularities (Rajopadhyaya et al., 1998). However, RWPs have large sampling volumes, coarse temporal resolution and provide winds from 1.5 km and beyond. Finally, Kollias et al. (2002) took advantage of the non-Rayleigh scattering signatures on 94-GHz radar Doppler spectra in rain to retrieve the vertical air motion. The aforementioned techniques certainly advanced our ability to retrieve V_{air} in deep convective clouds with heavy precipitation; however, these methods do not apply to warm shallow cloud systems with light precipitation (e.g., drizzling stratocumulus and shallow convection).

Here, the lower-bound method (Battan, 1964), the first proposed radar Doppler spectra technique for the estimation of V_{air} is revisited. According to this method, an assumption is made about the minimum drop size present in the radar scanning volume. This minimum size corresponds to a minimum fall speed, usually taken to be around 1 m s^{-1}. The difference between the assumed slower falling Doppler spectrum edge and that observed with the radar is the vertical air motion. Several factors limit the lower-bound method, particularly the sensitivity of the radar, the noise level of the Doppler spectrum, and the turbulence broadening of the spectrum. In this study, the technique is applied in warm phase clouds using a sensitive mm-wavelength radar; thus, the smallest particles are cloud droplets that have negligible fall velocity (Luke & Kollias, 2013). This eliminates the uncertainty introduced by the radar's sensitivity. In addition, we rely on improved estimates of the turbulence broadening (Borque et al., 2016) and on well-established techniques for the removal of the spectral broadening due to turbulence, wind shear, and the radar beam width (Shupe et al., 2008). The aforementioned advantages were implemented in the Shupe et al. (2008) study; however, the estimates of V_{air} showed a persistent bias when compared to aircraft measurements, indicating the need for an additional correction. Here, the bias of the estimated V_{air} is corrected by considering the influence of signal-to-noise ratio (SNR) on spectral broadening. We will demonstrate this influence using numerical simulations and provide the correction factor as a function of SNR and turbulence. The uncertainty of the proposed V_{air} retrieval technique is demonstrated using case studies and statistical comparisons. Finally, some preliminary results are presented to show the potential application of the retrieval product.

2. Instruments and Data

The data used in this study were collected at the U.S. Department of Energy Atmospheric Radiation Measurement (ARM) Eastern North Atlantic (ENA) observatory at Graciosa Island on the Azores archipelago. The primary instrument used in this study is the Ka-band ARM Zenith Radar (KAZR; Kollias et al., 2016). The KAZR is a vertically pointing 35-GHz cloud radar with a 30 m range and 2 s temporal resolution. It records the radar Doppler spectrum in 256 FFT bins with a Nyquist velocity of ±6 m s^{-1}. Postprocessing algorithms are used to estimate noise (Hildebrand & Sekhon, 1974), SNR, and several Doppler moments. In addition to original spectra data, the Microscale Active Remote Sensing of Clouds (MicroARSCL) product (Kollias et al., 2007b) will be used in this study to identify the spectral upward edge location. For this study, positive velocity always represents upward motion. In addition, observations from a profiling Doppler Lidar (DL) are used. The DL operates at a wavelength of 1.5 μm and is able to measure high precision wind velocity with an uncertainty below 0.2 m s^{-1} (Frehlich, 2001). Finally, we use Liquid Water Path (LWP) estimates from the Microwave Radiometer (MWR) with an uncertainty of 20–30 g m^{-2} (Turner et al., 2007).

Besides the observational products, independent retrievals are also used in the algorithm. The turbulence induced radar Doppler spectrum broadening σ_t is estimated using the methodology described in Borque et al. (2016). In the subcloud layer, drizzle microphysical retrievals are estimated using the radar-lidar technique developed by O'Connor et al. (2005). A detailed description of the drizzle retrievals used in this study can be found in Lamer and Kollias (2019). Finally, the V_{air} in the subcloud layer is estimated from the difference between the observed Doppler velocity and the reflectivity-weighted drizzle sedimentation velocity.

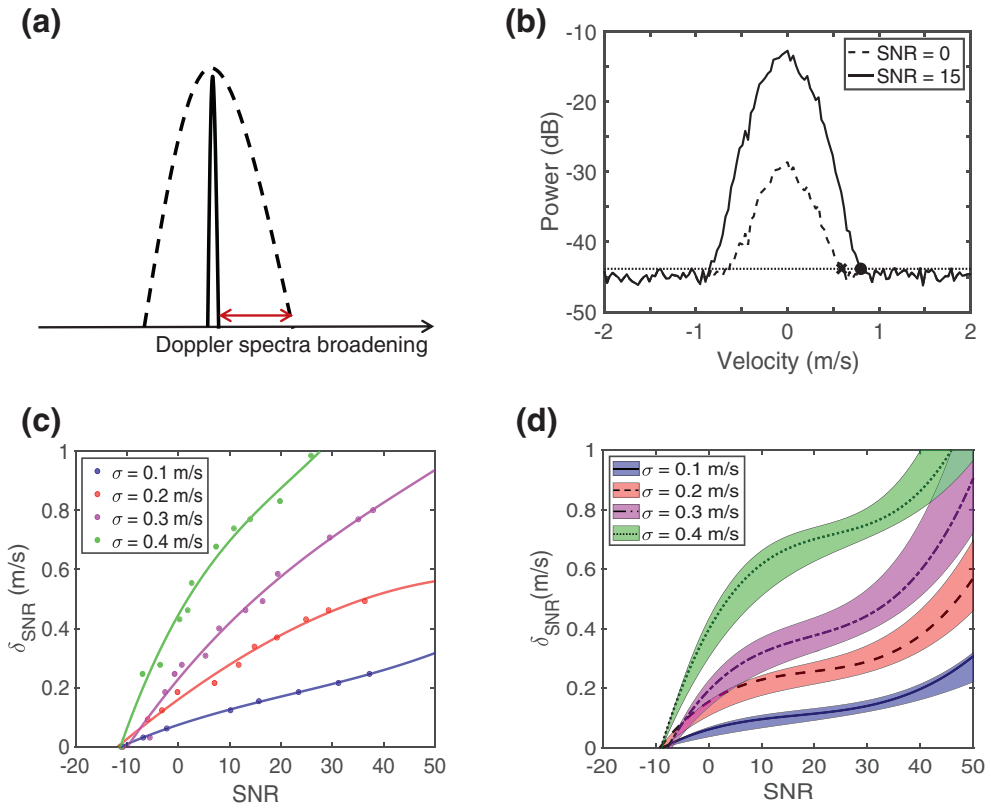

Figure 1. (a) Illustration of Doppler spectrum broadening, solid line represents Doppler spectrum of cloud droplets, dash line represents cloud Doppler spectrum with broadening effect. (b) Generated cloud spectra with SNR equals 0 (dashed line) and 15 (solid line), cross and solid circle indicates upward edge location of two spectra. (c) Cloud-only scenario: SNR broadening factor as a function of SNR for σ of 0.1 m s^{-1} (blue), 0.2 m s^{-1} (red), 0.3 m s^{-1} (magenta), 0.4 m s^{-1} (green), respectively. (d) Same as (c) but for cloud drizzle mixing scenario. Solid line, dashed line, dash-dot line, and dotted line represents the SNR broadening correction term with σ of 0.1 m s^{-1}, 0.2 m s^{-1}, 0.3 m s^{-1}, and 0.4 m s^{-1}, the shading area indicates uncertainty.

3. Methodology

Cloud droplets have negligible sedimentation velocities (e.g., 0.03 m s^{-1} for a 10-μm diameter droplet), and in nonturbulent conditions, their radar Doppler spectra will resemble a very narrow delta function-like spectral peak (solid line in Figure 1a). The location of this spectral peak in the recorded radar Doppler spectrum is the vertical air motion. However, due to the presence of turbulence and wind shear, the contribution of the observed cloud droplets to the radar Doppler spectrum is broader (dashed line in Figure 1a). In this study, we first propose that besides turbulence and wind shear, SNR also significantly modulates upward edge broadening and should be corrected in the retrieval algorithm. Thus, the vertical air motion can be obtained from the spectrum upward edge as:

$$V_{\text{air}} = V_{\text{edge}} - \sigma_t - \sigma_s - \delta_{SNR} \quad (1)$$

where σ_t and σ_s are the turbulence and wind shear broadening factors estimated using the Borque et al. (2016) methodology. δ_{SNR} is the SNR broadening factor and will be demonstrated and estimated in the following section. It is noted that spectrum broadening due to radar beam width, estimated as 0.03 m s^{-1}, is smaller than the other terms by an order of magnitude and is thus neglected in the algorithm.

3.1. Influence of SNR on Spectrum Upward Edge

A radar Doppler spectrum simulator was developed by Kollias et al. (2011) to generate Doppler spectra once the shape of Particle Size Distribution (PSD), Liquid Water Content (LWC), median volume diameter (D_0),

effective radius of cloud/drizzle droplets, and turbulence broadening (σ_t) are provided. This simulator is used to demonstrate the SNR effect on the velocity difference between the Doppler spectrum edge (V_{edge}) and V_{air}. Figure 1b shows two radar Doppler spectra generated using the same turbulence broadening σ_t of 0.2 m s^{-1} but with different SNR values (0 and 15 dB, dashed and solid lines, respectively). The two radar Doppler spectra are generated using the same cloud Particle Size Distribution (PSD) shape (lognormal) and effective radius (10 μm), and the different SNR values are generated by increasing the total cloud Liquid Water Content (LWC). The high-SNR Doppler spectrum has a 0.2 m s^{-1} more upward V_{edge} compared to the low SNR Doppler spectrum. Considering that the cloud PSD broadening effect is negligible for both simulated radar Doppler spectra and that we used the same turbulence broadening, the disagreement of upward edge is then due to the SNR broadening effect.

The SNR broadening effect on V_{edge} is explored using extensive forward radar Doppler spectra simulations with a range of SNR from −10 to +50 dB for given σ_t values of 0.1, 0.2, 0.3, and 0.4 m s^{-1}. For each σ_t scenario, a total of 10,000 Doppler spectra are generated with various SNR values. We assume the SNR broadening can be ignored for the smallest SNR (i.e., SNR = −10 dB). The SNR broadening term (δ_{SNR}) for larger SNR is calculated as the velocity displacement of the upward edge of the simulated Doppler spectra from that of the minimum SNR value (i.e., SNR = −10 dB) for a given σ_t value. The relationship between SNR and δ_{SNR} for different σ_t is shown in Figure 1c (solid circles). A third-order polynomial function was used to fit scatter for each turbulence scenario; second-order and fourth-order polynomials were also tried but turned out to result in either underfitting or overfitting (Figure S1). The aforementioned forward simulations are conducted using only cloud PSDs where the SNR changes with corresponding changes in LWC. Two distinct characteristics are evident in Figure 1c: (1) for the same turbulence, δ_{SNR} increases with SNR, corresponding to the SNR broadening effect; (2) for the same SNR value, δ_{SNR} also differs according to turbulence, indicating SNR broadening is also related to turbulence. Both of these dependences will be considered in the retrieval algorithm.

For a typical mm-wavelength radar, cloud detections rarely exceed +15 dB; thus, the assumed high-SNR cloud scenario in Figure 1c merely aims to show the effect of SNR broadening on cloud droplets without drizzle influence. Next, the analysis is extended to include a combination of cloud and drizzle PSDs. In the simulation, the cloud LWC varies between 0 and 1.0 g m^{-3} with a step of 0.005 g m^{-3}, the cloud effective radius is fixed to be 10 μm and the drizzle LWC is set to be 10% of the cloud LWC. The final drizzle input parameter in the simulator is the drizzle median volume diameter (D_0). The input D_0 is estimated using the following iterative process. A first estimate of D_0 is obtained using a D_0-LWC drizzle relationship, using the radar/lidar-based drizzle retrievals in the subcloud layer (black line in Figure S2). The initial D_0 estimate is used to predict the reflectivity-weighted drizzle sedimentation velocity V_{dr}. Finally, V_{dr} is used to update D_0 using the $V_{dr} - D_0$ relationship derived from the subcloud layer drizzle retrievals (black line in Figure S3). The updated D_0 along with other drizzle and cloud input parameters are used to generate the radar Doppler spectrum of the cloud and drizzle mixture. Following the same procedure used in the case of cloud-only simulations, the δ_{SNR} is calculated and fitted with a third-order polynomial function with SNR for each turbulence scenario (black lines in Figure 1d). It can be seen that δ_{SNR} increases quickly when SNR is small, as the cloud peak signal continues to grow and pushes the edge away. Once SNR exceeds 10, the drizzle signal begins to expand but not enough to affect the upward edge; thus, the black line becomes flat. After SNR exceeds 30, the drizzle signal starts to influence the spectrum edge and δ_{SNR} grows quickly again. Similar to the cloud scenario, δ_{SNR} increases with turbulence for a given SNR, which indicates δ_{SNR} should again be determined jointly by SNR and turbulence. δ_{SNR} can be described as a function of SNR for each turbulence category as follows:

$$\delta_{SNR} = \begin{cases} 0.061 + 0.005 \times SNR - 1.96 \times 10^{-4} \times SNR^2 + 3.88 \times 10^{-6} \times SNR^3, \sigma_t \le 0.1 m/s \\ 0.154 + 0.011 \times SNR - 4.84 \times 10^{-4} \times SNR^2 + 8.44 \times 10^{-6} \times SNR^3, 0.1 < \sigma_t \le 0.2 m/s \\ 0.192 + 0.018 \times SNR - 7.16 \times 10^{-4} \times SNR^2 + 1.26 \times 10^{-5} \times SNR^3, 0.2 < \sigma_t \le 0.3 m/s \\ 0.39 + 0.032 \times SNR - 1.2 \times 10^{-3} \times SNR^2 + 1.668 \times 10^{-5} \times SNR^3, 0.3 < \sigma_t \end{cases}$$

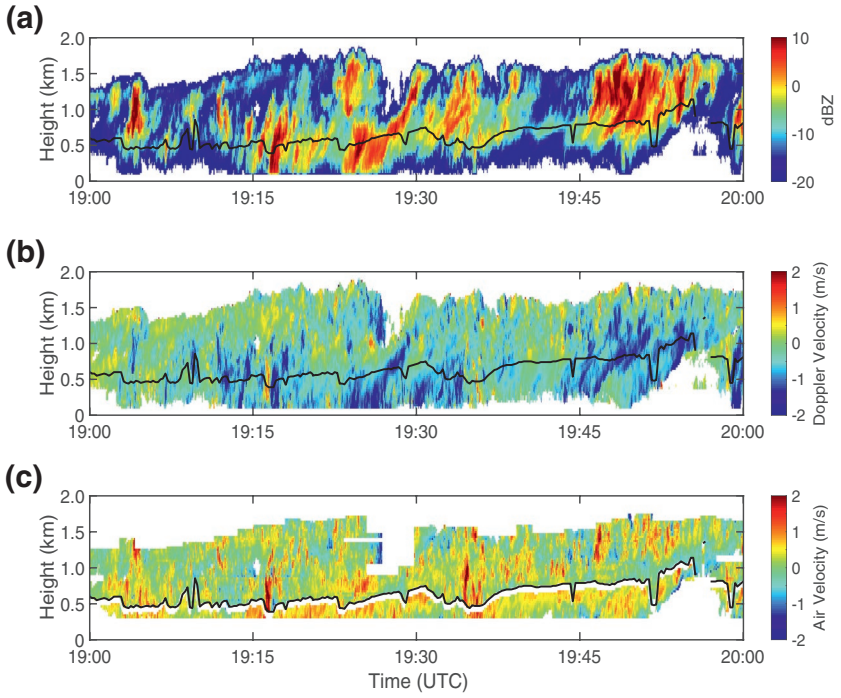

Figure 2. (a) Reflectivity, (b) Doppler velocity from KAZR, and (c) combined air velocity retrieval on 20170618 at ENA site. Black line represents cloud base determined by ceilometer. In (c), air velocity above cloud base is retrieved form the proposed technique, below cloud base is independent retrieval based on Radar-Lidar technique. Positive velocity represents upward motion.

3.2. Uncertainty Estimation

The uncertainty in the V_{air} estimation depends on how accurately we can estimate the radar Doppler spectrum broadening terms. The uncertainty of the SNR broadening term (δ_{SNR}) is mainly derived from the LWC partitioning between cloud and drizzle in the spectral simulations. To estimate this effect, sensitivity tests were applied by setting drizzle LWC to be 5%, 10%, 15%, and 20% of the cloud LWC. δ_{SNR} was fitted with SNR for each LWC setting and the resulting distribution, shown as the shaded area in Figure 1d, attributed to uncertainty. It shows the uncertainty also grows with SNR, and is bounded by 0.1 m s^{-1} for SNR smaller than 30, after which the uncertainty increases rapidly as the strong drizzle signal starts to control V_{edge}. Considering that the uncertainty of σ_t was around 0.1 m s^{-1}, the accuracy of retrieved air velocity was safely estimated to be 0.2 m s^{-1} for SNR smaller than 30.

4. Evaluation of the V_{air} Retrievals

The proposed V_{air} retrieval technique has been applied to 1 year of observations (2016) at the ARM ENA site. The quality of the retrievals has been evaluated using case studies of several hours duration and statistically using independent retrievals or observations. In case-based evaluations of the technique, the vertical air motion below the cloud base from the radar-lidar technique (O'Connor et al., 2005) is compared to the vertical air motion retrievals above the cloud base using the proposed technique.

Figure 2 shows an example of precipitating boundary layer clouds observed at ENA on 18 June 2017. The reflectivity and doppler velocity in the first two rows are characteristic of a typical cumulus case. Figure 2c shows the combined air velocity above cloud base from the spectrum technique of this study and the independent velocity retrieval in the subcloud layer. As the drizzle retrieval is applied starting from three range gates below cloud base to eliminate range gates with a mixture of cloud and drizzle, there is a blank space below cloud base. These two products show good consistency around cloud base, with the strong upward motions at around 19:05, 19:15, and 19:35 UTC seen in both retrievals having similar magnitude. A strong upward/downward air motion core is seen in the retrieval at 19:45 UTC, which is consistent with the char-

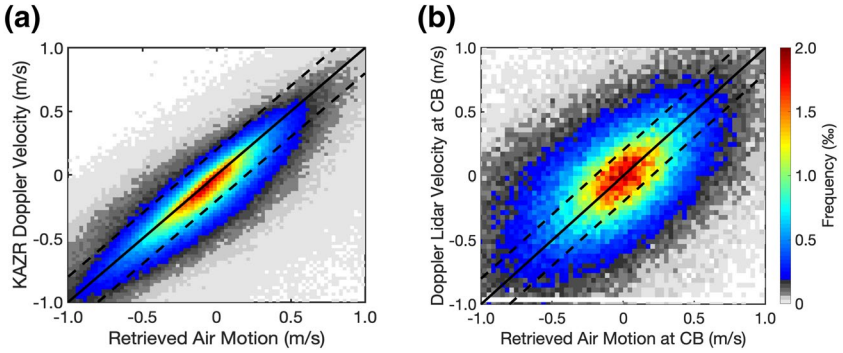

Figure 3. (a) Comparison between air velocity retrieval and in-cloud Doppler velocity from KAZR for drizzle-free cloud (dBZ < −20). (b) Comparison between air velocity retrieval and Doppler velocity from DL at cloud base. The color indicates the occurrences frequency per range bin normalized by the total observable number represented by permillage. Solid line is the one-to-one line and the dashed line represents the retrieval uncertainty.

acteristics of shallow cumuli described by Kollias et al. (2001). There are also inconsistencies between the two: at 19:50, the retrieved air velocity from the spectrum technique seems to underestimate the V_{air} compared with subcloud air velocity, which may be attributed to the uncertainty of the drizzle retrieval. Overall, the continuity of vertical air motion near cloud base indicates a fairly reliable ability of the technique to retrieve air motion in cumulus clouds.

The statistical evaluation is based on two different independent data sets. First, in drizzle-free clouds (dBZ < −20), the retrieved V_{air} is compared to the mean KAZR Doppler velocity (Figure 3a), which is a very good estimator of the vertical air motion in cases limited to drizzle-free conditions (Kollias et al., 2001). Figure 3a suggests that we can provide an unbiased estimate of the position of the peak of cloud droplets in the Doppler spectrum (hence the vertical air motion). This has not been demonstrated before. Although this is not a direct validation of the vertical air motion retrieval in drizzling conditions, it does provide validation for a significant component of the proposed technique. Second, as the DL is often used as a benchmark to validate vertical air velocity at cloud base (Endo et al., 2019), retrieved V_{air} is also compared to the observed vertical air motion from the DL at cloud base, as shown as Figure 3.

In both comparisons, the retrieval agrees with observations fairly well and shows no systematic bias. Sixty-four percentage of the difference between the V_{air} retrieval and Doppler velocity from the KAZR are bounded by the 0.2 m s^{-1} uncertainty shown as the dashed lines (Figure 3a). Forty-two percentage difference of the V_{air} and DL velocity at cloud base are within the retrieval uncertainty (dashed lines in Figure 3b). This comparison indicates that the proposed technique is able to properly account for the Doppler spectrum broadening. Moreover, the retrieval without SNR correction, i.e., ignoring δ_{SNR} in Equation 1, and the spectrum upward edge (V_{edge} in Equation 1) are also compared with observations of KAZR Doppler velocity and DL cloud base velocity (Figure S4). The overestimated V_{air} retrieval in the comparison with the two data sets (Figures S4a and S4c) indicates SNR broadening correction is necessary for the retrieval algorithm. An interesting finding is that a strong positive correlation between spectrum upward edge and DL observed velocity, although biased due to spectral broadening, is robust evidence to support the retrieval assumption: spectrum upward edge velocity V_{edge} is closely related to the vertical air motion.

5. Vertical Air Motion Statistics in Low Clouds

The retrieved V_{air} can be used to improve drizzle microphysical retrievals above the cloud base (i.e., Frisch et al., 1995) and to characterize the in-cloud dynamics. The latter is usually limited to nonprecipitating clouds with dBZ less than a threshold value (i.e., −17) to ensure that cloud droplets control the radar moments (Ghate et al., 2010; Lamer et al., 2015). The proposed technique is not limited to the presence of drizzle and small raindrops and can thus be applied to all warm clouds. Here, vertical air motion statistics from one entire year of ENA observations of warm, low-level clouds is shown in Figure 4. The majority of the low-level clouds used are stratiform. The statistics are presented in three Liquid Water Path (LWP)

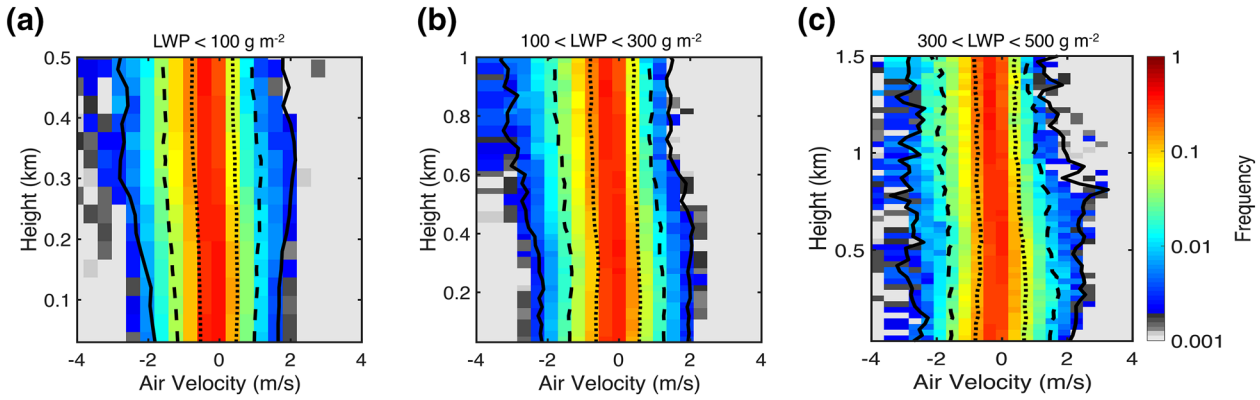

Figure 4. Air velocity distribution for (a) LWP smaller than 100 g m^{-2}, (b) 100 g m^{-2} < LWP < 300 g m^{-2}, and (c) 300 g m^{-2} < LWP < 500 g m^{-2}. The color represents the occurrences frequency per range bin normalized horizontally. Solid line, dashed line, and dot line represents 99%, 95%, and 75% of upward (positive velocity) and downward (negative velocity) air motion, respectively.

categories (0–100; 100–300; and 300–500 g m^{-2}). These three categories correspond to clouds with different cloud thickness. The vertical coordinate is distance above the cloud base height. At each height, the normalized probability density function of the retrieved V_{air} is shown. The solid, dashed, and dotted lines represent the 99%, 95%, and 75% of upward (positive velocity) and downward (negative velocity) air motion, respectively.

The mean vertical air motion profiles exhibit near-zero mean and the majority of the vertical air motions are within ±1 m s^{-1}. This is consistent with the assertion that the majority of the clouds are stratiform. On the other hand, cumulus clouds are characterized by stronger updraft and downdraft motions; however, their significantly lower cloud fraction results in less V_{air} estimates. One noticeable difference among the V_{air} retrievals in the three LWP regimes is the profile of the 99% updraft and downdraft velocities. For the low LWP regime (<100 g m^{-2}), the strongest upward and downward velocities are found near the cloud top. This is consistent with higher turbulence near the cloud top and the plausible role of a cloud-top radiative cooling mechanism in maintaining these shallow stratiform layers. In the middle LWP category (100–300 g m^{-2}), the strongest downdrafts are near the cloud top while the maximum updrafts are found lower in the cloud layer, suggesting cloud base (cumulus) convection (solid line in Figure 4b). This transition is completed for the highest LWP regime where the strongest updrafts and downdrafts reach ±3 m s^{-1}.

6. Conclusions

A new warm-cloud air vertical velocity retrieval algorithm is proposed based on KAZR-observed Doppler spectra. The novel aspect is the validation that SNR also contributes to spectral edge broadening besides turbulence and wind shear, and should be corrected in order to retrieve nonbiased air velocities. Spectral simulation of cloud-only scenarios is applied to demonstrate the SNR broadening effect, the results suggesting that the SNR broadening term increases with SNR and also depends on the turbulence being simulated. SNR broadening factor in the mixed cloud and drizzle scenario is estimated via numerical simulations with appropriate parameter settings. After correcting all the broadening terms from the spectrum upward edge, air vertical velocity can be retrieved with an uncertainty of 0.2 m s^{-1} for SNR smaller than 30.

Case and statistical comparisons are applied to verify the retrieved V_{air}. For one cumulus case verification, the retrieved air motion in cloud is consistent with the independent air velocity retrieval in the subcloud layer. The comparison also shows that the retrieval successfully captures the typical upward/downward structure in cumulus clouds. One year of statistical comparisons with KAZR and DL observations shows our velocity retrieval is reliable and the SNR correction is the final piece of the puzzle needed to correct for the traditional bias of the V_{air} retrieval based on the lower-bound method. Overall, the verification demonstrates the reliability and accuracy of the retrieval algorithm and provides opportunities for the future applications.

One year of V_{air} retrievals are analyzed to provide a first, general investigation of the vertical air motion distribution in cloud with different LWP categories. The analysis indicates that with increasing LWP values, stronger updrafts and downdrafts are retrieved, especially near the cloud base. On the other hand, clouds with small LWP tend to have stronger upward/downward motion near cloud top. Future applications of the retrieved V_{air} include improved drizzle microphysical retrievals above the cloud base and investigations on the role of cloud dynamics on precipitation initiation.

Data Availability Statement

The ground-based remote sensing data used in this study can be downloaded from ARM data archive site: https://adc.arm.gov/discovery/.

Acknowledgments
Z. Zhu contributions were supported by the U.S. Department of Energy (DOE) ASR ENA Site Science award. P. Kollias, F. Yang, and E. Luke were supported by the U.S. DOE under contract DE-SC0012704.

References

Ansmann, A., Fruntke, J., & Engelmann, R. (2010). Updraft and downdraft characterization with Doppler lidar: Cloud-free versus cumuli-topped mixed layer. *Atmospheric Chemistry and Physics*, *10*(16), 7845–7858.

Battan, L. J. (1964). Some observations of vertical velocities and precipitation sizes in a thunderstorm. *Journal of Applied Meteorology*, *3*(4), 415–420.

Blyth, A. M., Lasher-Trapp, S. G., & Cooper, W. A. (2005). A study of thermals in cumulus clouds. *Quarterly Journal of the Royal Meteorological Society: A*, *131*(607), 1171–1190.

Borque, P., Luke, E., & Kollias, P. (2016). On the unified estimation of turbulence eddy dissipation rate using Doppler cloud radars and lidars. *Journal of Geophysical Research: Atmospheres*, *121*(10), 5972–5989. https://doi.org/10.1002/2015JD024543

Bretherton, C. S., McCaa, J. R., & Grenier, H. (2004). A new parameterization for shallow cumulus convection and its application to marine subtropical cloud-topped boundary layers. Part I: Description and 1D results. *Monthly Weather Review*, *132*(4), 864–882.

Delanoe, J., Protat, A., Bouniol, D., Heymsfield, A., Bansemer, A., & Brown, P. (2007). The characterization of ice cloud properties from Doppler radar measurements. *Journal of Applied Meteorology and Climatology*, *46*(10), 1682–1698. https://doi.org/10.1175/jam2543.1

de Roode, S. R., Siebesma, A. P., Jonker, H. J., & de Voogd, Y. (2012). Parameterization of the vertical velocity equation for shallow cumulus clouds. *Monthly Weather Review*, *140*(8), 2424–2436.

Donner, L. J., O'Brien, T. A., Rieger, D., Vogel, B., & Cooke, W. F. (2016). Are atmospheric updrafts a key to unlocking climate forcing and sensitivity? *Atmospheric Chemistry and Physics*, *16*(20), 12983–12992.

Endo, S., Zhang, D., Vogelmann, A. M., Kollias, P., Lamer, K., Oue, M., et al. (2019). Reconciling differences between large-eddy simulations and Doppler lidar observations of continental shallow cumulus cloud-base vertical velocity. *Geophysical Research Letters*, *46*(20), 11539–11547. https://doi.org/10.1029/2019GL084893

Frehlich, R. (2001). Estimation of velocity error for Doppler lidar measurements. *Journal of Atmospheric and Oceanic Technology*, *18*(10), 1628–1639.

Frisch, A. S., Fairall, C. W., & Snider, J. B. (1995). Measurement of stratus cloud and drizzle parameters in ASTEX with a Ka-band Doppler radar and a microwave radiometer. *Journal of the Atmospheric Sciences*, *52*(16), 2788–2799.

Ghate, V. P., Albrecht, B. A., & Kollias, P. (2010). Vertical velocity structure of nonprecipitating continental boundary layer stratocumulus clouds. *Journal of Geophysical Research*, *115*, D13204. https://doi.org/10.1029/2009JD013091

Gossard, E. E. (1994). Measurement of cloud droplet size spectra by Doppler radar. *Journal of Atmospheric and Oceanic Technology*, *11*(3), 712–726.

Hildebrand, P. H., & Sekhon, R. (1974). Objective determination of the noise level in Doppler spectra. *Journal of Applied Meteorology*, *13*(7), 808–811.

Kalesse, H., & Kollias, P. (2013). Climatology of high cloud dynamics using profiling ARM Doppler radar observations. *Journal of Climate*, *26*(17), 6340–6359. https://doi.org/10.1175/jcli-d-12-00695.1

Kollias, P., Albrecht, B. A., Lhermitte, R., & Savtchenko, A. (2001). Radar observations of updrafts, downdrafts, and turbulence in fair-weather cumuli. *Journal of the Atmospheric Sciences*, *58*(13), 1750–1766.

Kollias, P., Albrecht, B. A., & Marks, F., Jr. (2002). Why Mie? Accurate observations of vertical air velocities and raindrops using a cloud radar. *Bulletin of the American Meteorological Society*, *83*(10), 1471–1484.

Kollias, P., Albrecht, B. A., & Marks, F. D., Jr. (2003). Cloud radar observations of vertical drafts and microphysics in convective rain. *Journal of Geophysical Research*, *108*(D2), 4053. https://doi.org/10.1029/2001JD002033

Kollias, P., Clothiaux, E. E., Ackerman, T. P., Albrecht, B. A., Widener, K. B., Moran, K. P., et al. (2016). Development and applications of ARM millimeter-wavelength cloud radars. *Meteorological Monographs*, *57*, 17.1–17.19.

Kollias, P., Clothiaux, E. E., Miller, M. A., Albrecht, B. A., Stephens, G. L., & Ackerman, T. P. (2007a). Millimeter-wavelength radars—New Frontier in atmospheric cloud and precipitation research. *Bulletin of the American Meteorological Society*, *88*(10), 1608–1624. https://doi.org/10.1175/bams-88-10-1608

Kollias, P., Clothiaux, E. E., Miller, M. A., Luke, E. P., Johnson, K. L., Moran, K. P., et al. (2007b). The Atmospheric Radiation Measurement Program cloud profiling radars: Second-generation sampling strategies, processing, and cloud data products. *Journal of Atmospheric and Oceanic Technology*, *24*(7), 1199–1214. https://doi.org/10.1175/jtech2033.1

Kollias, P., Remillard, J., Luke, E., & Szyrmer, W. (2011). Cloud radar Doppler spectra in drizzling stratiform clouds: 1. Forward modeling and remote sensing applications. *Journal of Geophysical Research*, *116,* D13201. https://doi.org/10.1029/2010jd015237

Korolev, A., & Isaac, G. (2003). Phase transformation of mixed-phase clouds. *Quarterly Journal of the Royal Meteorological Society: A*, *129*(587), 19–38.

Lamer, K., & Kollias, P. (2015). Observations of fair-weather cumuli over land: Dynamical factors controlling cloud size and cover. *Geophysical Research Letters*, *42*, 8693–8701. https://doi.org/10.1002/2015gl064534

Lamer, K., & Kollias, P. (2019). Characterization of shallow oceanic precipitation using profiling and scanning radar observations at the Eastern North Atlantic ARM observatory. *Atmospheric Measurement Techniques*, *12*(9), 4931–4947.

Lamer, K., Kollias, P., & Nuijens, L. (2015). Observations of the variability of shallow trade wind cumulus cloudiness and mass flux. *Journal of Geophysical Research: Atmospheres*, *120*(12), 6161–6178. https://doi.org/10.1002/2014JD022950

Lareau, N. P., Zhang, Y., & Klein, S. A. (2018). Observed boundary layer controls on shallow cumulus at the ARM Southern Great Plains site. *Journal of the Atmospheric Sciences*, *75*(7), 2235–2255.

Luke, E. P., & Kollias, P. (2013). Separating cloud and drizzle radar moments during precipitation Onset using Doppler spectra. *Journal of Atmospheric and Oceanic Technology*, *30*(8), 1656–1671. https://doi.org/10.1175/jtech-d-11-00195.1

O'Connor, E. J., Hogan, R. J., & Illingworth, A. J. (2005). Retrieving stratocumulus drizzle parameters using Doppler radar and lidar. *Journal of Applied Meteorology*, *44*(1), 14–27.

Park, S.-B., Gentine, P., Schneider, K., & Farge, M. (2016). Coherent structures in the boundary and cloud layers: Role of updrafts, subsiding shells, and environmental subsidence. *Journal of the Atmospheric Sciences*, *73*(4), 1789–1814.

Protat, A., & Williams, C. R. (2011). The accuracy of radar estimates of ice terminal fall speed from vertically pointing Doppler radar measurements. *Journal of Applied Meteorology and Climatology*, *50*(10), 2120–2138. https://doi.org/10.1175/jamc-d-10-05031.1

Radenz, M., Buhl, J., Lehmann, V., Gorsdorf, U., & Leinweber, R. (2018). Combining cloud radar and radar wind profiler for a value added estimate of vertical air motion and particle terminal velocity within clouds. *Atmospheric Measurement Techniques*, *11*(10), 5925–5940. https://doi.org/10.5194/amt-11-5925-2018

Rajopadhyaya, D. K., May, P. T., Cifelli, R. C., Avery, S. K., Willams, C. R., Ecklund, W. L, & Gage, K. S. (1998). The effect of vertical air motions on rain rates and median volume diameter determined from combined UHF and VHF wind profiler measurements and comparisons with rain gauge measurements. *Journal of Atmospheric and Oceanic Technology*, *15*(6), 1306–1319.

Shupe, M. D., Kollias, P., Poellot, M., & Eloranta, E. (2008). On deriving vertical air motions from cloud radar Doppler spectra. *Journal of Atmospheric and Oceanic Technology*, *25*(4), 547–557. https://doi.org/10.1175/2007jtecha1007.1

Takahashi, H., Suzuki, K., & Stephens, G. (2017). Land–ocean differences in the warm-rain formation process in satellite and ground-based observations and model simulations. *Quarterly Journal of the Royal Meteorological Society*, *143*(705), 1804–1815.

Telford, J., & Warner, J. (1962). On the measurement from an aircraft of buoyancy and vertical air velocity in cloud. *Journal of the Atmospheric Sciences*, *19*(5), 415–423.

Turner, D. D., Clough, S. A., Lijegren, J. C., Clothiaux, E. E., Cady-Pereira, K. E., & Gaustad, K. L. (2007). Retrieving liquid water path and precipitable water vapor from the atmospheric radiation measurement (ARM) microwave radiometers. *IEEE Transactions on Geoscience and Remote Sensing*, *45*(11), 3680–3690. https://doi.org/10.1109/tgrs.2007.903703

Wakasugi, K., Mizutani, A., Matsuo, M., Fukao, S., & Kato, S. (1986). A direct method for deriving drop-size distribution and vertical air velocities from VHF Doppler radar spectra. *Journal of Atmospheric and Oceanic Technology*, *3*(4), 623–629. https://doi.org/10.1175/1520-0426(1986)003<0623:admfdd>2.0.co;2

Wang, Z., French, J., Vali, G., Wechsler, P., Haimov, S., Rodi, A., et al. (2012). Single aircraft integration of remote sensing and in situ sampling for the study of cloud microphysics and dynamics. *Bulletin of the American Meteorological Society*, *93*(5), 653–668.

Williams, C. R. (2012). Vertical air motion retrieved from dual-frequency profiler observations. *Journal of Atmospheric and Oceanic Technology*, *29*(10), 1471–1480. https://doi.org/10.1175/jtech-d-11-00176.1